

Signaling Pathways from Cannabinoid Receptor-1 Activation to Inhibition of *N*-Methyl-D-Aspartic Acid Mediated Calcium Influx and Neurotoxicity in Dorsal Root Ganglion Neurons

Qing Liu, Manjunatha Bhat, Wayne D. Bowen, and Jianguo Cheng

Departments of Pain Management and Neurosciences, Anesthesiology Institute and Lerner Research Institute, Cleveland Clinic, Cleveland, Ohio (Q.L., M.B., J.C.); and Department of Molecular Pharmacology, Physiology, and Biotechnology, Brown University, Providence, Rhode Island (W.D.B.)

Received May 14, 2009; accepted September 10, 2009

ABSTRACT

Although the activation of cannabinoid receptor-1 (CB1) receptors by cannabinoids is known to inhibit neuronal hyperexcitability and reduce excitotoxic cell death, the mechanistic links between these two actions remain elusive. We tested the hypothesis that activation of CB1 receptors inhibits *N*-methyl-D-aspartic acid (NMDA)-mediated calcium influx and cell death via the inositol triphosphate (IP₃) signaling pathway in both primary dorsal root ganglia neurons and a cultured neuronal cell line (F-11 cells). These cells were pretreated with the cannabinoid agonist (*R*)-(+)-[2,3-dihydro-5-methyl-3-(4-morpholinylmethyl)pyrrolo[1,2,3-de]-1,4-benzoxazin-6-yl]-1-naphthalenylmethanone (*R*-(+)-WIN 55,212-2; WIN) before exposure to NMDA. Concentrations of cytosolic calcium were measured with the ratiometric calcium indicator, Fura-2, and cell death was determined by a cell viability test. WIN dose-dependently attenuated both the calcium influx and cell death induced by NMDA. These effects were blocked by selective cannabinoid CB1 receptor antagonists *N*-(piperidin-1-yl)-5-(4-chlorophenyl)-1-(2,4-dichlorophenyl)-4-methyl-1*H*-pyrazole-3-carbox-

amide (SR141716A) or *N*-(piperidin-1-yl)-5-(4-iodophenyl)-1-(2,4-dichlorophenyl)-4-methyl-1*H*-pyrazole-3-carboxamide (AM251), but not CB2 receptor antagonist *N*-[(1*S*)-endo-1,3,3-trimethylbicyclo[2.2.1]heptan-2-yl]-5-(4-chloro-3-methylphenyl)-1-(4-methyl-benzyl)-pyrazole-3-carboxamide (SR144528). It is interesting to note that a transient Ca²⁺ signal was observed after the acute application of WIN. This Ca²⁺ increase was blocked by a CB1 receptor antagonist AM251, IP₃ receptor antagonist 2-aminoethyl diphenylborinate, or by depleting intracellular Ca²⁺ stores with the endoplasmic reticulum Ca²⁺ pump inhibitor thapsigargin. Removal of extracellular Ca²⁺, on the other hand, had no effect on the CB1 receptor-induced Ca²⁺ increase. These data suggest that WIN triggers a cascade of events: it activates the CB1 receptor and the IP₃ signaling pathway, stimulates the release of Ca²⁺ from intracellular stores, raises the cytosolic Ca²⁺ levels, and inhibits the NMDA-mediated Ca²⁺ influx and cell death through a process that remains to be determined.

This work was supported by the National Institutes of Health National Institute of Neurological Disorders and Stroke [Grant 1 R01-NS052372] (to J.C.).

Parts of this work were previously presented in abstract form as follows: Cheng J, Liu Q, and Bhat M (2008) Cannabinoid *R*-(+)-WIN 55,212-2 inhibits NMDA-induced Ca²⁺ influx and cell death in dorsal root ganglion neurons. *6th Forum of European Neurosciences*; 2008 Jul 12-16; Geneva, Switzerland. Abstract, vol. 4, 115.2, The Swiss Society for Neuroscience, Geneva, Switzerland; Cheng J, Liu Q, Bhat BM, and Bowen WD (2007) Attenuation of NMDA-induced Ca²⁺ rise by cannabinoid receptors in primary sensory neurons; 2007 Nov 3-7; San Diego, CA. Abstract 33, 821.11, Society for Neuroscience, Washington, DC.

Article, publication date, and citation information can be found at <http://jpet.aspetjournals.org>.
doi:10.1124/jpet.109.156216.

Cannabinoid receptors are members of the superfamily of G_i/G_o-coupled receptors and include at least two subtypes, Cannabinoid receptor-1 (CB1) and CB2 receptors. The CB1 receptor is expressed primarily in the central nervous system (Matsuda et al., 1990) and peripheral nociceptors (Agarwal et al., 2007), whereas the CB2 receptor is predominantly expressed in immune cells (Munro et al., 1993) and is also detectable in brainstem neurons (Van Sickle et al., 2005) and spinal cord (Zhang et al., 2003). More recently, another cannabinoid receptor GPR55 was identified that appears to be highly expressed in large dorsal root ganglion neurons

ABBREVIATIONS: CB1, cannabinoid receptor-1; NMDA, *N*-methyl-D-aspartic acid; PKA, protein kinase A; IP₃, inositol triphosphate; *R*-(+)-WIN 55,212-2, (*R*)-(+)-[2,3-dihydro-5-methyl-3-(4-morpholinylmethyl)pyrrolo[1,2,3-de]-1,4-benzoxazin-6-yl]-1-naphthalenylmethanone; WIN, *R*-(+)-WIN 55,212-2; DRG, dorsal root ganglia; AM251, *N*-(piperidin-1-yl)-5-(4-iodophenyl)-1-(2,4-dichlorophenyl)-4-methyl-1*H*-pyrazole-3-carboxamide; SR141716A, *N*-(piperidin-1-yl)-5-(4-chlorophenyl)-1-(2,4-dichlorophenyl)-4-methyl-1*H*-pyrazole-3-carboxamide; SR144528, *N*-[(1*S*)-endo-1,3,3-trimethylbicyclo[2.2.1]heptan-2-yl]-5-(4-chloro-3-methylphenyl)-1-(4-methyl-benzyl)-pyrazole-3-carboxamide; DMSO, dimethyl sulfoxide; TG, thapsigargin; DPBS, Dulbecco's phosphate-buffered saline; 2-APB, 2-aminoethyl diphenylborinate; XTT, 2,3-Bis(2-methoxy-4-nitro-5-sulfophenyl)-2*H*-tetrazolium-5-carboxanilide; ER, endoplasmic reticulum; SERCA, sarco/endoplasmic reticulum Ca²⁺ pump; HEK, human embryonic kidney.

(Lauckner et al., 2008). The CB1 receptor is involved in the integration of signals from both lipid- and peptide-derived signaling molecules. The two lipid endogenous agonists, anandamide and 2-arachidonoylglycerol, are well characterized and are derived from cell membrane lipids (Boyd, 2006; Di Marzo and Petrosino, 2007). In contrast, the two peptide endogenous agonists, RVD-Hp α and VD-Hp α , are newly discovered (Gomes et al., 2009) and are derived from the precursor α -hemoglobin, which is extensively expressed in many cell types including neurons and glia (Richter et al., 2009), in addition to erythrocytes. Previous studies have shown that cannabinoid receptor activation leads to the inhibition of adenylyl cyclase activity, inhibition of calcium channels, and D-type potassium channels, increases in the phosphorylation of mitogen-activated protein kinases, and activation of A-type and inwardly rectifying potassium channels (Pertwee, 1997; Howlett and Mukhopadhyay, 2000; Pertwee and Ross, 2002). The endocannabinoid system is proposed to have important roles in many pathophysiological processes including Parkinson's disease, Alzheimer's disease, atrophic lateral sclerosis, multiple sclerosis, obesity, depression, inflammation, and neuropathic pain (Iversen and Chapman, 2002; Boyd, 2006; Di Marzo and Petrosino, 2007).

CB1 receptor agonists protect neurons from *N*-methyl-D-aspartic acid (NMDA)-induced excitotoxicity in *in vitro* experiments (van der Stelt and Di Marzo, 2005). The cellular mechanisms underlying the CB1 receptor-mediated neuroprotection may include inhibition of the presynaptic release of glutamate (Shen and Thayer, 1998), inhibition of NMDA-induced intracellular Ca²⁺ release (Zhuang et al., 2005), antioxidant activity (Marsicano et al., 2002), protein kinase A (PKA) signaling, and nitric oxide generation (Kim et al., 2006). Activation of CB1 receptors also protects cultured spinal neurons from the cytotoxic effects of excitatory amino acids (Abood et al., 2001). The cannabinoid-mediated neuroprotection was used as a therapeutic approach to manage neurodegenerative conditions such as multiple sclerosis (Docagne et al., 2007). However, the mechanisms by which the cannabinoids protect spinal neurons remain elusive.

It is well established that excessive Ca²⁺ influx through NMDA channels triggers cytotoxic cell death in neurons, and suppression of the Ca²⁺ influx can protect cells from NMDA-induced cytotoxicity. In addition, the roles of NMDA receptor activation in the development of persistent neuropathic pain have been demonstrated previously (Woolf, 1983; Woolf and Salter, 2000). Cannabinoids may modulate NMDA-induced Ca²⁺ influx in different neurons through different mechanisms. The NMDA-induced Ca²⁺ increase was inhibited by a CB1 receptor-mediated membrane hyperpolarization in rat cortical and cerebellar slices (Hampson et al., 1998). In primary hippocampal cells, CB1 receptor activation was capable of inhibiting the calcium release, in a cAMP/PKA-dependent manner, from ryanodine-sensitive intracellular store (Zhuang et al., 2005). In contrast, CB1 receptor activation increased NMDA-evoked Ca²⁺ release from inositol triphosphate (IP₃)-sensitive intracellular store in cerebellar granule neurons (Netzeband et al., 1999). Therefore, cannabinoids may enhance or inhibit the NMDA-induced increase in Ca²⁺ levels depending on the cell type, the type of cannabinoid ligands, and the subsequent signaling pathways activated.

In this study, we examined the effects of cannabinoid *R*-(+)-WIN 55,212-2 (WIN) on NMDA-induced cytotoxicity

and NMDA-evoked Ca²⁺ influx. These experiments were carried out in dorsal root ganglia (DRG) neurons and murine F-11 cells (spinal DRG \times neuroblastoma hybrid), both of which express CB1 receptors and NMDA receptors. We tested the hypothesis that activation of cannabinoid CB1 receptors inhibits NMDA-mediated calcium influx and cell death via the IP₃ signaling pathway in both primary DRG neurons and cultured F-11 cells. We chose these two types of cells with different pharmacology for the release of calcium from intracellular stores so that we could identify the signaling pathways of WIN-induced calcium increase. Although both cell types are able to produce IP₃ receptor-mediated Ca²⁺ signals, only DRG neurons are sensitive to stimulation with ryanodine receptor activator, caffeine, and express functional ryanodine receptors. The F-11 cells do not respond to caffeine, indicating that these cells lack endogenous ryanodine receptors (Yankura et al., 2003).

Materials and Methods

Cell Culture. All procedures used in the animal experiments were approved by the Institutional Animal Care and Use Committee of Cleveland Clinic Foundation. DRG neurons were obtained as described earlier (Dedov et al., 2001). In brief, DRG isolated from adult Sprague-Dawley rats (200–300 g) were incubated in Hanks' balanced saline solution (Invitrogen, Carlsbad, CA) with 0.05% collagenase and 0.25% trypsin for 25 min at 37°C. Neurons were dissociated by trituration of ganglia with fire-polished Pasteur pipettes of decreasing diameter, and afterward the cellular suspension was washed twice in Dulbecco's modified Eagle's medium supplemented with 10% fetal calf serum and 2 mM L-glutamine. Freshly isolated neurons were plated onto collagen-coated coverslips and cultured in Dulbecco's modified Eagle's medium/F-12 Ham media containing 2 mM L-glutamine supplemented with 10% fetal bovine serum, HAT supplement (100 μ M hypoxanthine, 400 nM aminopterin, 16 μ M thymidine), 50 ng/ml nerve growth factor, 100 units/ml penicillin, and 100 μ g/ml streptomycin. Cells were kept under 5% CO₂ at 37°C and passed twice a week using nonenzymatic cell dissociation solution.

F-11 cells (purchased from Dr. Mark C. Fishman, Massachusetts General Hospital, MA) were cultured in F-12 Ham media containing 2 mM L-glutamine supplemented with 15% fetal bovine serum, HAT supplement, 100 units/ml penicillin and 100 μ g/ml streptomycin. Cells were kept under 5% CO₂ at 37°C and passed twice a week using nonenzymatic cell dissociation solution.

Cells were visualized by using bright-field illumination at 20 \times magnification on a Leica DMIRB inverted microscope (Leica Microsystems, Inc., Deerfield, IL). The images of the cells were captured 24 h before and after drug treatment by using a CCD video camera and QCapture Pro imaging software from QImaging (Surrey, BC, Canada).

Compound Preparation. WIN 55,212-2 and AM251 were purchased from BIOMOL International LP (Plymouth Meeting, PA). SR141716A and SR144528 were provided by the National Institute on Drug Abuse. Compounds were dissolved in 100% dimethyl sulfoxide (DMSO) as a 10 mM stock and diluted with Dulbecco's phosphate-buffered saline (DPBS; Invitrogen) to their final concentrations. Final concentrations of 10, 50, 100, and 500 nM of WIN 55,212-2 were used to activate CB1 receptors. SR141716A and AM251 were used at a final concentration of 500 nM to block CB1 receptor activation, and SR144528 was used at a final concentration at 500 nM to block CB2 receptor activation. NMDA (Sigma-Aldrich, St. Louis, MO) was dissolved in DPBS as a 10 mM stock. The final concentration of 100 μ M NMDA was used to elicit Ca²⁺ signals. Thapsigargin (TG) (Research Biochemical, Natick, MA) was prepared as a 10 mM stock solution in DMSO. Final concentration of 150

nM TG was used in the experiments. 2-Aminoethyl diphenylborinate (2-APB) (Sigma-Aldrich) was prepared as a 1 mM stock solution in DMSO, and a final concentration of 100 μ M was used in the experiments. Stock solutions were stored at -20°C . All dilutions of stock were prepared fresh before addition to the culture medium. All vehicles were confirmed to have no biological effects.

Cytotoxicity Analysis. Cells were plated in poly-D-lysine-coated 96-well plates at a density of 10^4 cells/well in their respective culture media. Cells were allowed to adhere for 12 h before the medium was replaced with Mg^{2+} and serum-free medium: DME/F-12 supplemented with 2% B27 (Sigma-Aldrich). Cell death was induced by incubating with 0.001 to 10 mM NMDA for 20 ± 2 h. To determine the effects of cannabinoids, cells were incubated with or without NMDA (100 μ M) in presence or absence of WIN 55,212-2 (10, 50, 100, 500 nM) for 24 h. To determine the cannabinoid receptor subtype specificity, cells were treated with SR141716A (500 nM) for 20 to 30 min before incubating with NMDA and WIN 55,212-2. In experiments where the effects of cannabinoids on intracellular calcium levels and cytotoxicity were investigated, cells were pretreated with 150 nM TG for 10 min, before cells were cocubated with cannabinoids and NMDA. The cell viability was assayed by measuring the conversion of a tetrazolium salt, 2,3-Bis(2-methoxy-4-nitro-5-sulphophenyl)-2H-tetrazolium-5-carboxanilide (XTT), into its formazan derivative by cellular dehydrogenases. The assay was performed according to the manufacturer's instruction (Trevigen TACS XTT Cell Proliferation Assay; Trevigen, Gaithersburg, MD). The absorbance was read on a VICTOR³V plate reader by using a 490-nm filter (PerkinElmer Life and Analytical Sciences, Waltham, MA). For each condition, four wells of cells were measured and the experiments were repeated three times ($n = 12$ for each condition). The cytotoxicity index (CI) was calculated as follows: $\text{CI} = (\text{control well absorbance} - \text{treatment well absorbance}) / (\text{control well absorbance} - \text{Triton-treated well absorbance})$.

Calcium Imaging. Cytosolic Ca^{2+} was monitored with the ratio-metric indicator Fura-2 (InCyt Im2 Dual-wavelength Fluorescence Imaging System; Intracellular Imaging, Cincinnati, OH). Cells were grown on glass coverslips coated with collagen (MatTek Corporation, Ashland, MA) and then washed twice in DPBS before incubation in 2 ml of DPBS containing 2.0 to 3.0 μ M Fura-2 AM and 0.066% Pluronic F-127 (Invitrogen). After incubating for 60 to 75 min at 37°C in darkness, cultures were washed twice in DPBS to remove extracellular dye and kept at room temperature in the dark for more than 30 min before use in the experiments. All measurements were performed in DPBS or, where specified, in Ca^{2+} -free DPBS. Drugs were added in a volume of 200 μ l to cells in 3 ml of DPBS to make the final volume less than 4 ml in the Petri dishes. The dishes with dye-loaded cells were mounted on the stage of Nikon TS-100 fluorescence inverted microscope with a Cohu model 4915 charge-coupled device (CCD) camera (Nikon, Melville, NY). Fluorescent images were captured alternately at the excitation wavelengths of 340 and 380 nm

with an emission wavelength of 520 nm, which were analyzed with InCyt Im2 version 4.62 imaging software (Intracellular Imaging).

A standard curve was used to derive experimental $[\text{Ca}^{2+}]_i$ values. The standard curve was generated by using various concentrations of Ca^{2+} (Calcium Calibration Buffer Kit) in the presence of indicator dye Fura-2 free acid (Invitrogen). During each experiment, background fluorescence was estimated for a region without cells, and this value was automatically subtracted from the measured emission of each channel. The F_{340}/F_{380} ratios of cell emissions were compared with the standard curve stored in the computer, and both the ratio and $[\text{Ca}^{2+}]_i$ were displayed on screen. Preliminary measurement of $[\text{Ca}^{2+}]_i$ was taken on various cells in the field before any drug application. Only cells with basal $[\text{Ca}^{2+}]_i$ in the range of 90 to 120 nM were chosen for the experiments described here.

Experimental Paradigm. All pharmacological agents were dissolved in DPBS and applied by brief microperfusion from micropipettes placed near the cells of interest. The concentration and duration (<2 s) of application were adjusted under control conditions for each experiment to produce Ca^{2+} signals with peak amplitude (150–350 nM) that could be easily quantified.

Ca^{2+} levels in the presence of TG and cannabinoids were typically measured 5 to 20 min after the initial drug exposure. NMDA was added 10 min after the responses returned to baseline. For a majority of the experiments, the bath saline (e.g., DPBS) used during control recordings contained DMSO concentration equivalent to that used in the presence of thapsigargin or cannabinoid agents. Separate vehicle control experiments showed that DMSO ($<0.15\%$) did not affect the measurements under study.

In general, Ca^{2+} levels at rest or in response to challenges were measured simultaneously for 10 to 30 cells within a microscopic field, with three to five microscopic fields measured per condition. One microscopic field was measured in each Petri dish. Each cell was tested under only one condition. Resting Ca^{2+} levels were subtracted from amplitude measurements for individual cells to yield peak Ca^{2+} values.

Data Analysis. A between-cell comparison was used to determine the effects of the tested compounds on Ca^{2+} levels or cytotoxicity. For each group of studies, data from at least five individual Petri dishes were pooled for summary analysis. Each drug was tested on at least two different days, with concurrent interleaved controls. Averages are reported as the mean \pm S.E.M., and the number of cells and/or cultures studied is given. Raw data were analyzed with appropriate parametric tests: paired or unpaired t test or analysis of variance (performed with SPSS software; SPSS Inc., Chicago, IL). When analysis of variance was used, post hoc analysis for group differences was performed by using Scheffe's F test or Dunn's test for unequal sample sizes. Statistical significance was determined at a significance level of $p < 0.05$.

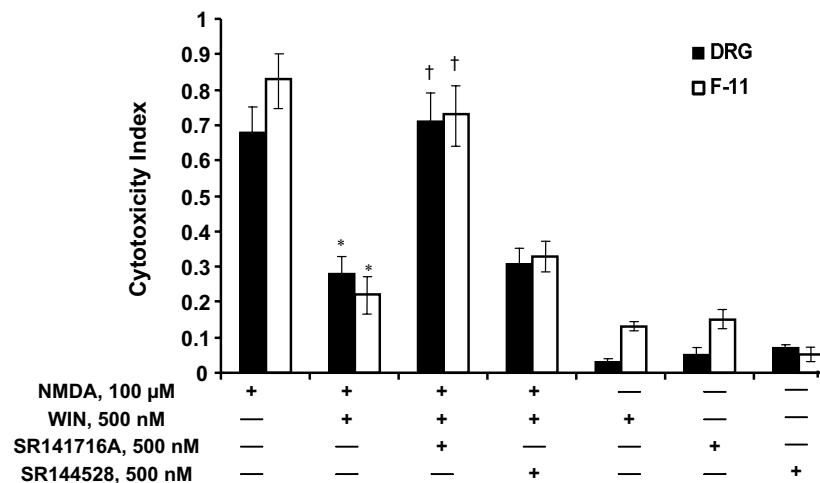


Fig. 1. Activation of CB1 receptors inhibits NMDA-induced cell death in DRG neurons and F-11 cells. Cells were exposed to NMDA (100 μ M) for 24 h in the absence or presence of cannabinoid receptor agonist *R*-(+)-WIN 55,212-2 (500 nM). NMDA reduced the viability of cells by approximately 70% for DRG neurons and 80% for F-11 cells in the absence of WIN. The NMDA-induced cytotoxicity was reduced significantly in the presence of WIN. This WIN-mediated protective effect was blocked by the CB1 receptor antagonist SR141716A (500 nM), but not the CB2 receptor antagonist SR144528 (500 nM). Cell survival was not affected by either WIN, SR141716A, or SR144528 alone. Cell death was measured by the cytotoxicity index, as defined under *Materials and Methods*. Data shown are means \pm S.E.M. for 20 wells per condition. *, $p < 0.05$ compared to treatment with NMDA alone, Scheffe's tests. †, $p < 0.05$ compared to NMDA + WIN condition.

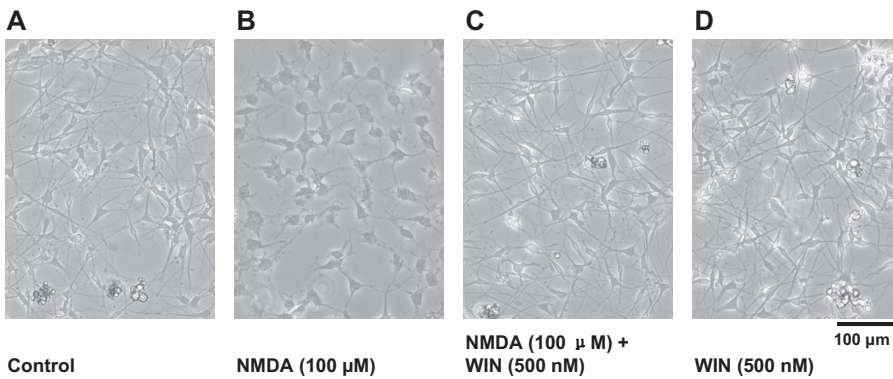


Fig. 2. WIN reduced NMDA-induced cytotoxicity. Representative examples of DRG neurons cultured in control medium without drugs (A), medium containing NMDA (100 μ M) (B), medium containing both NMDA (100 μ M) and WIN (500 nM) (C), and medium containing WIN (500 nM) (D) for 24 h.

Results

Cannabinoid *R*-(+)-WIN Inhibited NMDA-Induced Cytotoxicity in Both DRG and F-11 Cells. Long-term treatment of both DRG and F-11 cells with NMDA (100 μ M) produced significant cytotoxic effects. A 24-h exposure to NMDA reduced the viability of the DRG neurons by \sim 70% and the viability of F-11 cells by \sim 80% (Fig. 1). These cytotoxic effects were blocked by adding the cannabinoid receptor agonist *R*-(+)-WIN (500 nM) to the culture medium ($F_{(1,19)} = 21.25$ for DRG neurons, $F_{(1,13)} = 12.16$ for F-11 cells, $p < 0.05$). The protective effects of WIN were reversed by CB1 receptor antagonist SR141716A (500 nM) ($F_{(1,18)} = 16.73$ for DRG neurons, $F_{(1,14)} = 9.61$ for F-11 cells, $p < 0.05$) but not by CB2 receptor antagonist SR144528 (500 nM) ($p > 0.05$), suggesting a specific CB1 receptor-mediated effect. Figure 2 shows representative microphotographs of DRG neuron cultures in control (Fig. 2A), treated with NMDA (100 μ M) (Fig. 2B), treated with the combination of NMDA (100 μ M) and WIN (500 nM) (Fig. 2C), or treated with WIN (500 nM) alone. After 24 h of drug treatment, DRG neurons exposed to NMDA exhibited signs of cytotoxicity that was prevented by treatment with WIN. The cytotoxicity of NMDA and the protective effects of WIN were quantified by using a commercial assay for cell viability and proliferation (see *Materials and Methods*).

WIN Dose-Dependently Inhibited the Ca^{2+} Rise Induced by NMDA. Many toxic effects of NMDA are mediated by increases in cytoplasmic Ca^{2+} levels ($[Ca^{2+}]_i$). Therefore, we examined the effects of *R*-(+)-WIN 55,212-2 on the NMDA-induced increase in $[Ca^{2+}]_i$. Figure 3A (Control) shows that NMDA (100 μ M) elicited an increase in $[Ca^{2+}]_i$ in DRG neurons. The NMDA-induced change in $[Ca^{2+}]_i$ was characterized by a relatively rapid initial rise in intracellular Ca^{2+} to a peak amplitude of \sim 600 nM that was followed by a slow recovery to baseline. All of the cells tested responded to NMDA (100 μ M). Ca^{2+} levels increased approximately 400% above baseline for both the DRG neurons and F-11 cells (Fig. 3B). Resting Ca^{2+} levels in DRG neurons and F-11 cells were fairly consistent within and between experimental trials and typically ranged from 85 to 105 nM.

The effects of WIN on the NMDA-elicited $[Ca^{2+}]_i$ increase were studied by pretreating cells with 10, 100, and 500 nM WIN 5 min before the application of NMDA (100 μ M). WIN produced a dose-dependent depression of the calcium rise elicited by NMDA over the entire testing period (Fig. 3A). Likewise, WIN also depressed NMDA-evoked $[Ca^{2+}]_i$ increase in F-11 cells in a dose-dependent manner (data not

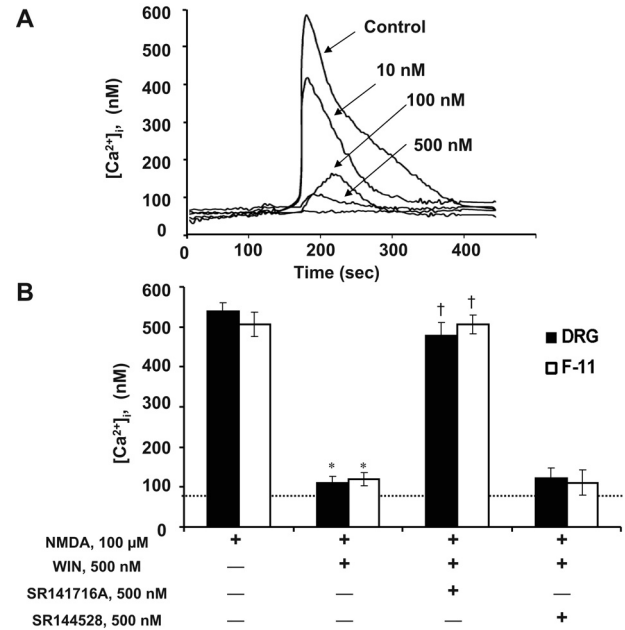


Fig. 3. CB1 receptor activation reduces NMDA-induced Ca^{2+} influx in DRG neurons and F-11 cells. Neurons were pretreated with WIN in the presence or absence of CB1 receptor antagonist SR141716A for 5 min before exposure to NMDA (100 μ M). A, representative Ca^{2+} signal recordings from DRG neurons show a dose-dependent inhibition of NMDA-induced Ca^{2+} signals by WIN pretreatment (10, 100, and 500 nM). The control is from cells treated with NMDA (100 μ M) alone. Ratios of wavelengths 340:380 nm were converted into calcium concentrations (nM) by using a standard curve as described under *Materials and Methods*. B, calcium concentrations increased by \sim 400% in response to NMDA (100 μ M) in both cell types. Coapplication of NMDA with WIN reduced Ca^{2+} signals by \sim 80%. The inhibition was reversed by CB1 receptor antagonist, SR141716A. A CB2 receptor antagonist SR144528 (500 nM) did not reduce the WIN-induced inhibition. The dotted line indicates the baseline calcium level. Values are averages from 10 to 15 cells \pm S.E.M. *, $p < 0.05$ compared to treatment with NMDA alone, Scheffe's tests. †, $p < 0.05$ compared to NMDA + WIN condition.

shown). Figure 3B shows pooled data for the effects of 500 nM WIN on the NMDA-evoked Ca^{2+} increase. The depression of NMDA-induced Ca^{2+} rise by WIN was observed in both DRG neurons and F-11 cells ($F_{(2,34)} = 7.69$ for DRG neurons, $F_{(2,18)} = 8.14$ for F-11 cells, $p < 0.05$ versus NMDA alone; Fig. 3B). The effects of WIN were reversed by pretreatment with the selective CB1 receptor antagonist, SR141716A (500 nM) ($F_{(1,34)} = 6.39$ for DRG neurons $F_{(1,21)} = 5.82$ for F-11 cells, $p < 0.05$ versus NMDA + WIN), but not by the CB2 antagonist SR144528 (500 nM) (Fig. 3B), suggesting that the effects of WIN were mediated by the CB1 receptors.

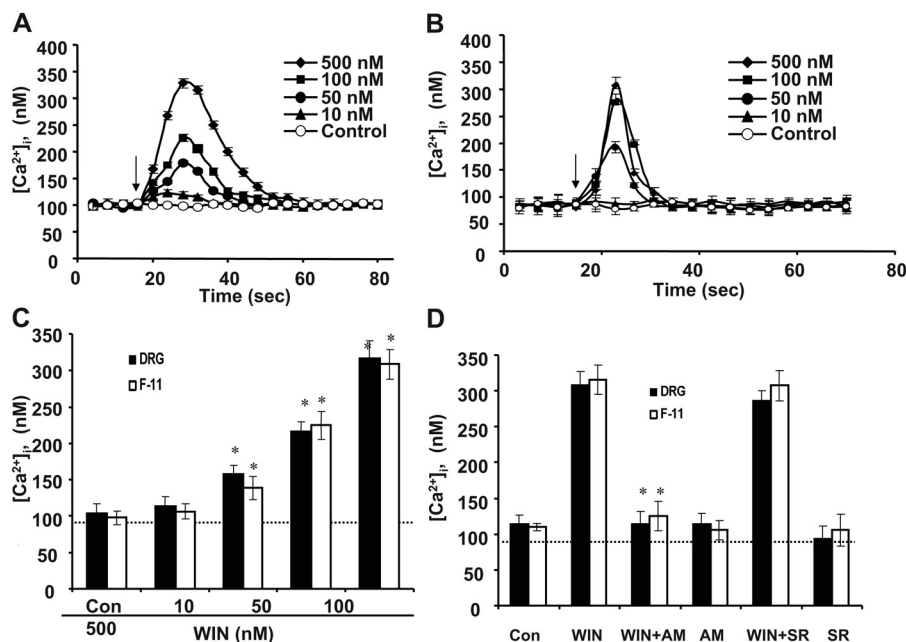


Fig. 4. Cannabinoid agonist WIN induces increases in $[Ca^{2+}]_i$. WIN produced a transient rise in $[Ca^{2+}]_i$ that began within seconds after application (arrows) and returned to baseline within 1 min in a dose-dependent manner for both DRG neurons (A) and F-11 cells (B). Each Ca^{2+} trace represents the mean \pm S.E.M. from 25 DRG neurons or 21 F-11 cells measured individually. Error bars are smaller than the corresponding symbols in many cases. Data were acquired at 4-s intervals throughout the entire experiments. C, average peak amplitudes in the $[Ca^{2+}]_i$ produced by WIN in both cell types. *, $p < 0.05$, compared to control (Con) by post hoc Scheffe's tests. D, CB1 receptor antagonist AM251 (AM; 500 nM) inhibited WIN-induced increase in $[Ca^{2+}]_i$, whereas the CB2 receptor antagonist SR144528 (SR; 500 nM) had little effect. AM251 alone had little effect on Ca^{2+} levels. *, $p < 0.05$ compared to WIN alone, Scheffe's tests. All experiments were conducted in normal DPBS. The dotted line indicates the baseline calcium level.

WIN-Evoked a Dose-Dependent Calcium Rise in Primary DRG Neurons and F-11 Cells. Cells were challenged with different concentrations of WIN (10, 50, 100, and 500 nM) while the intracellular Ca^{2+} levels were monitored. WIN-evoked a dose-dependent intracellular calcium rise in both DRG neurons (Fig. 4A) and F-11 cells (Fig. 4B). Ca^{2+} signals increased upon WIN application, peaked within 30 s, and returned to baseline within 2 min (Fig. 4, A and B). This transient calcium increase was observed in 92% DRG neurons and 87% F-11 cells. Figure 4C shows that the average peak amplitudes of WIN-induced calcium rise was dose-dependent ($F_{(3,34)} = 8.07$ for DRG neurons, $F_{(3,25)} = 6.14$ for F-11 cells, $p < 0.05$ versus Control; Fig. 4C). The calcium rise induced by WIN was blocked by the CB2 antagonist AM251 (500 nM) but not the CB2 antagonist SR144528 (500 nM; Fig. 4D), suggesting that it was mediated by CB1 receptors in both DRG neurons and F-11 cells [$F_{(1,33)} = 9.73$ for DRG neurons, $F_{(1,22)} = 6.58$ for F-11 cells, $p < 0.05$ versus WIN treatment (500 nM); Fig. 4D]. AM251 and SR144528 did not significantly change $[Ca^{2+}]_i$ for either cell type ($p > 0.05$).

Sources of the WIN- and NMDA-Induced Calcium Increase. The WIN- and NMDA-induced increase in $[Ca^{2+}]_i$ could come from either an extracellular calcium source or from intracellular calcium stores such as the endoplasmic reticulum (ER). Influx of extracellular calcium was assessed by using a calcium-free medium (0 Ca^{2+} DPBS). Release from intracellular calcium store was determined by depleting ER stores with a sarco/endoplasmic reticulum Ca^{2+} (SERCA) pump inhibitor, TG, before NMDA or WIN challenge. WIN-induced $[Ca^{2+}]_i$ increase (Fig. 5A, Con) was significantly reduced by pretreatment of both DRG neurons and F-11 cells with TG [$F_{(1,18)} = 10.56$ for DRG neurons, $F_{(1,16)} = 9.33$ for F-11 cells, $p < 0.05$ versus WIN treatment (500 nM)], whereas removal of extracellular calcium (Ca^{2+} , 0 nM) did not affect the signals ($p > 0.05$; Fig. 5A). These data suggest that Ca^{2+} released from the ER contributes to the WIN-induced calcium increase. Pretreating cells with TG for 15 min in 0 Ca^{2+} DPBS has been shown to be sufficient to deplete TG-sensitive intracellular calcium stores (Chen et al.,

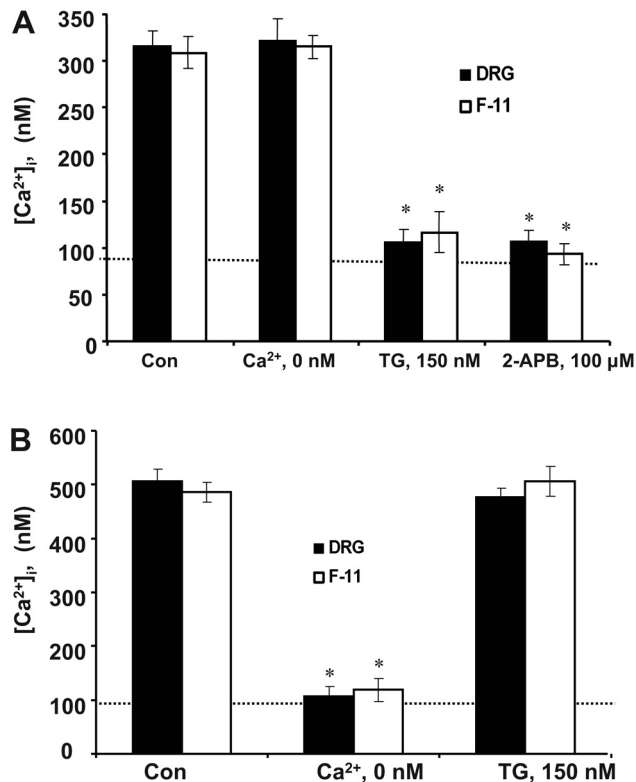


Fig. 5. Sources of cytosolic calcium rise. A, WIN-induced Ca^{2+} signals are from release of intracellular calcium stores in both DRG and F-11 cells. Cells were treated with thapsigargin (150 nM) or 2-APB (100 μ M) for 5 min to deplete or block release from intracellular Ca^{2+} stores. The application of TG or 2-APB before WIN abolished the calcium rise. In contrast, the removal of extracellular Ca^{2+} (Ca^{2+} , 0 nM) from DPBS did not affect the WIN-induced Ca^{2+} signals. Values are averages from 15 to 20 cells \pm S.E.M. B, NMDA-induced Ca^{2+} signals are from extracellular calcium sources. Removal of extracellular Ca^{2+} (Ca^{2+} , 0 nM) from DPBS abolished the NMDA-induced Ca^{2+} rise, whereas pretreatment with thapsigargin did not reduce the Ca^{2+} signals. *, $p < 0.05$ compared to control. The dotted line indicates the baseline calcium level.

2005). The ability of thapsigargin to deplete the intracellular Ca^{2+} stores was tested by stimulating Ca^{2+} release from IP_3 -sensitive stores with a type 1 muscarinic receptor agonist, carbachol (Cruzblanca et al., 1998). We found that the same thapsigargin treatment almost abolished the Ca^{2+} increase produced by 1 mM carbachol (data not shown). In contrast, the NMDA-evoked $[\text{Ca}^{2+}]_i$ increase (Fig. 5B, Con) was not affected by thapsigargin (Fig. 5B). Instead, it was significantly reduced by removal of extracellular calcium (Ca^{2+} , 0 nM), suggesting that the $[\text{Ca}^{2+}]_i$ evoked by NMDA comes from an influx of extracellular calcium, at least initially ($F_{(1,17)} = 5.89$ for DRG neurons, $F_{(1,14)} = 7.24$ for F-11 cells, $p < 0.05$ versus NMDA alone; Fig. 5B).

We further tested the role of IP_3 signaling pathway in the cannabinoid-evoked intracellular calcium release. Cells were pretreated with IP_3 receptor blocker, 2-APB (100 μM), for 5 min before they were exposed to WIN (500 nM). Pretreatment with 2-APB reduced the WIN-evoked calcium release in both DRG neurons and F-11 cells ($F_{(1,17)} = 6.47$ for DRG neurons, $F_{(1,12)} = 5.83$ for F-11 cells, $p < 0.05$ versus WIN treatment; Fig. 5A). These results suggest that the cannabinoid-induced increase in $[\text{Ca}^{2+}]_i$ was mediated by IP_3 receptors.

WIN-Induced Calcium Release Is Related to Its Inhibition of the NMDA-Mediated Ca^{2+} Influx. We tested whether the WIN-induced $[\text{Ca}^{2+}]_i$ increase was necessary to depress the NMDA-induced Ca^{2+} influx. DRG neurons and F-11 cells were preincubated with TG or 2-APB to inhibit the WIN-evoked increase in $[\text{Ca}^{2+}]_i$, before exposure to NMDA. Application of thapsigargin (150 nM) caused a robust transient rise in $[\text{Ca}^{2+}]_i$ in DRG neurons, which is indicative of intracellular calcium store depletion (Fig. 6B). After the $[\text{Ca}^{2+}]_i$ returned to baseline, application of 500 nM WIN did

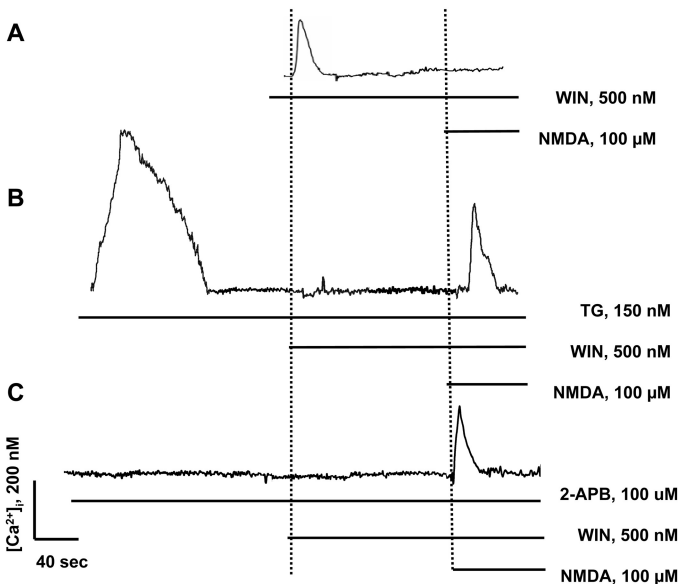


Fig. 6. WIN-induced intracellular calcium release is required to block NMDA-mediated calcium influx in DRG neurons. A, WIN blocked NMDA-induced calcium rise. B, depletion of intracellular calcium store with TG inhibited the ability of WIN to block the NMDA-induced calcium rise. C, inhibition of intracellular calcium release by 2-APB-mediated inactivation of IP_3 receptors also inhibited the ability of WIN to block the NMDA-induced calcium rise. These representative examples of Ca^{2+} signals were recorded continuously during pharmacological challenges of DRG neurons in DPBS ($n = 17$ cells). The vertical and horizontal lines indicate the beginning and duration of the drug applications.

not produce rises in $[\text{Ca}^{2+}]_i$ in DRG neurons, whereas the subsequent application of NMDA produced near normal Ca^{2+} increase. Similar results were seen in F-11 cells (data not shown). The differential effects of thapsigargin on the modulation of Ca^{2+} levels by WIN and NMDA are summarized in Fig. 7A. For both DRG neurons and F-11 cells, thapsigargin inhibited the WIN-induced Ca^{2+} increase ($F_{(1,34)} = 9.66$ for DRG neurons, $F_{(1,21)} = 7.45$ for F-11 cells, $p < 0.05$ versus NMDA alone; Fig. 7A), but not the NMDA (100 μM)-elicited Ca^{2+} rise ($F_{(1,24)} = 8.74$ for DRG neurons, $F_{(1,15)} = 6.27$ for F-11 cells, $p < 0.05$ versus NMDA + WIN; Fig. 7A). These results suggest that TG abolished the ability of WIN to inhibit the NMDA-induced Ca^{2+} influx and that Ca^{2+} release from intracellular stores was therefore required for this effect.

Likewise, the WIN-induced depression of NMDA-mediated calcium influx was blocked by the IP_3 receptor blocker, 2-APB (100 μM), in DRG neurons and F-11 cells (Figs. 6C and 7B). Pretreatment with 2-APB before WIN application abolished the WIN-evoked intracellular Ca^{2+} rise ($F_{(1,28)} = 7.53$ for DRG neurons, $F_{(1,18)} = 6.92$ for F-11 cells; $p < 0.05$ versus WIN alone; Fig. 7B). In addition, 2-APB blocked the WIN-induced inhibition of NMDA-mediated Ca^{2+} influx ($F_{(1,23)} = 11.32$ for DRG neurons, $F_{(1,19)} = 9.53$ for F-11 cells, $p < 0.05$ versus NMDA + WIN; Fig. 7B). These data suggest that WIN-induced $[\text{Ca}^{2+}]_i$ release is mediated by the IP_3 signaling pathway and is responsible for the inhibition of NMDA-mediated Ca^{2+} influx.

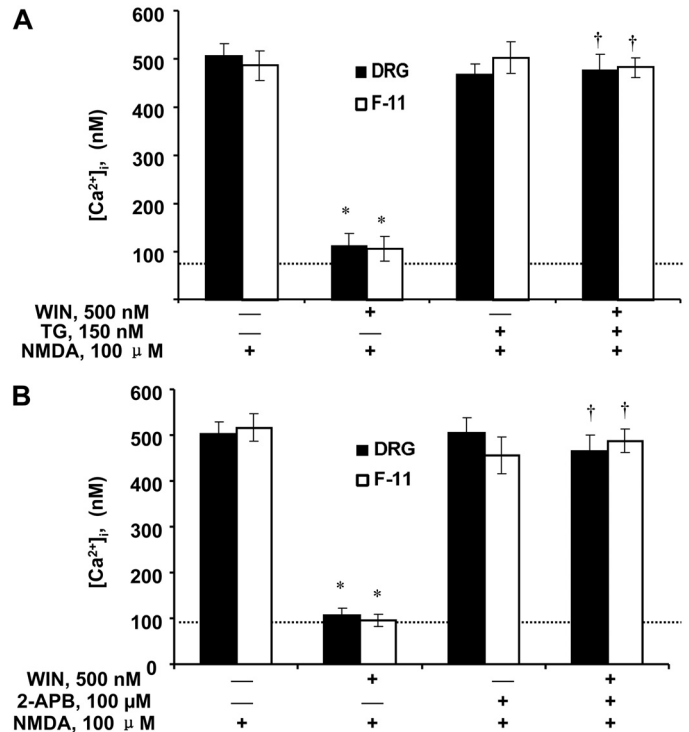


Fig. 7. Depression of intracellular calcium release prevents WIN from blocking NMDA-induced calcium influx in both DRG neurons and F-11 cells. A, pretreatment with SERCA pump inhibitor TG prevented WIN from blocking NMDA-induced calcium rise in both DRG neurons and F-11 cells. B, pretreatment with IP_3 receptor inhibitor 2-APB prevented WIN from blocking NMDA-induced Ca^{2+} signals in both cell types. Note, neither thapsigargin nor 2-APB alone produced any effect on NMDA-induced Ca^{2+} increase. *, $p < 0.05$ compared to NMDA treatment alone. †, $p < 0.05$ compared to NMDA + WIN treatment condition. The dotted line indicates the baseline calcium level.

WIN-Induced Ca^{2+} Release Is Responsible for the Inhibition of NMDA-Induced Cytotoxicity. We tested whether WIN-induced Ca^{2+} release is necessary for the protective effects of WIN on NMDA-evoked cytotoxicity in both DRG and F-11 cells. Coincubation of WIN (500 nM) with NMDA (100 μM) blocked the NMDA-induced cytotoxicity in both DRG and F-11 cells ($F_{(1,34)} = 33.96$ for DRG neurons, $F_{(1,24)} = 19.55$ for F-11 cells, $p < 0.05$ versus NMDA alone; Figs. 1 and 8). This protective effect was reversed by thapsigargin (150 nM) for both cell types ($F_{(1,42)} = 41.66$ for DRG neurons, $F_{(1,27)} = 34.19$ for F-11 cells, $p < 0.05$ versus NMDA + WIN; Fig. 7). These data suggest that WIN-induced $[\text{Ca}^{2+}]_i$ rise is required for WIN to protect cells from NMDA-induced cytotoxicity. Thapsigargin alone did not produce any significant cell viability ($<30\%$ for both cell types, $p > 0.05$).

Discussion

The data from this study showed that the cannabinoid *R*-(+)-WIN 55,212-2 produced a CB1-mediated neuroprotection against NMDA-induced cytotoxicity in both primary DRG neurons and F-11 cells. These effects were blocked by a SERCA pump inhibitor, thapsigargin, and an IP_3 receptor inhibitor, 2-APB, suggesting that Ca^{2+} release from intracellular stores via the IP_3 signaling pathway is critical for the CB1-mediated neuroprotection (Fig. 8). This work is the first demonstration that the IP_3 signaling pathway has been implicated in the cannabinoid-induced neuroprotection of spinal neurons.

The biochemical mechanisms of cannabinoid protection from NMDA-induced neuronal cytotoxicity are just beginning to be understood. It has been shown that WIN protects neurons against NMDA toxicity by activation of CB1 receptor and downstream inhibition of PKA signaling and nitric oxide generation in cultured cortical neurons (Kim et al., 2006). A natural extract from cannabis plant, Δ^9 -tetrahydrocannabinol, functions as an antioxidant to increase cell survival in NMDA-induced neurotoxicity in a mesencephalic cell line (Chen et al., 2005). In contrast, the data of this study indicate that the cannabinoid-mediated neuroprotection from NMDA-induced cytotoxicity in spinal neurons is largely attributable

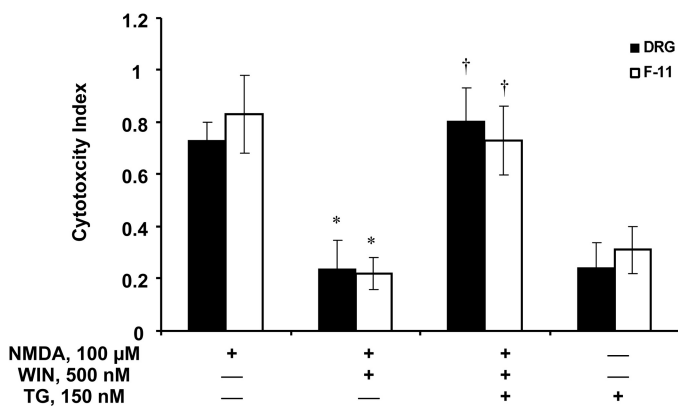


Fig. 8. The neuroprotective effects of CB1 activation are dependent on calcium release from intracellular stores. Depletion of intracellular calcium stores with SERCA pump inhibitor TG prevented WIN from inhibiting NMDA-induced cytotoxicity in both DRG neurons and F-11 cells. Note, thapsigargin alone did not affect the survival of cells. Data are means \pm S.E.M. from 23 wells per condition. *, $p < 0.05$ compared to NMDA alone. †, $p < 0.05$ compared to NMDA + WIN condition.

to its suppression of NMDA-induced Ca^{2+} influx through the IP_3 signaling pathway. We demonstrated that blocking CB1 receptor activation or the subsequent increase in $[\text{Ca}^{2+}]_i$ abolished the cannabinoid-mediated inhibition of Ca^{2+} influx and cytotoxicity induced by NMDA in primary DRG neurons. We also confirmed these findings for the F-11 cells.

The NMDA-induced cytosolic Ca^{2+} increase in spinal neurons could come from either an influx of extracellular Ca^{2+} through NMDA receptor ion channels and voltage-gated calcium channels (Reichling and MacDermontt, 1993) or from release of intracellular Ca^{2+} stores (Qiu et al., 1995). The data of this study suggest that activation of CB1 receptors primarily inhibits the influx of extracellular Ca^{2+} . Removal of extracellular Ca^{2+} significantly reduced NMDA-mediated cytosolic Ca^{2+} signals, whereas the SERCA pump inhibitor thapsigargin, in contrast, did not affect the NMDA-induced calcium increase. Therefore, the CB1-mediated inhibition of the Ca^{2+} increase in these neurons is probably due to inactivation of NMDA receptor channels and/or voltage-gated calcium channels. It has been shown that cannabinoids inhibit NMDA-elicited Ca^{2+} signals by blocking voltage-gated calcium channels in rat brain cerebellar and cortical slices (Hampson et al., 1998). However, it remains to be determined whether this is the case in the DRG neurons.

An interesting finding of this study is that the cannabinoid-mediated suppression of NMDA-induced Ca^{2+} influx depended on Ca^{2+} release from intracellular stores. CB1-mediated Ca^{2+} release from intracellular stores has been demonstrated in hippocampal neurons (Lauckner et al., 2005) and other cell types. The Ca^{2+} release was thought to be mediated through either $\text{G}_{\text{y/o}} \beta\gamma$ or G_q -coupled phospholipase C signaling pathway, depending on the cell types and drug concentrations. For example, WIN induced Ca^{2+} signals from IP_3 -sensitive ER stores in hippocampal neurons and transfected HEK293 cells (Lauckner et al., 2005). The data of this study are consistent with this finding. The short duration of Ca^{2+} signal surge (<40 s) observed in these experiments, compared with the reported long-lasting Ca^{2+} rise (>100 s), may be due to differences in WIN concentrations. A relatively low concentration (500 nM) was used in the experiments of this study, whereas high doses (5 μM) were used by others.

We demonstrated in this study that the CB1-induced calcium release from intracellular stores attenuated NMDA-induced Ca^{2+} influx, and subsequently the NMDA-induced cytotoxicity in DRG neurons. This finding is consistent with the reports that increases in $[\text{Ca}^{2+}]_i$ inactivates NMDA receptors in spinal dorsal horn neurons (Kyrozis et al., 1996) and hippocampal neurons (Kotecha and MacDonald, 2003). The NMDA receptor inactivation in response to increase in $[\text{Ca}^{2+}]_i$ was mediated by activation of Ca^{2+} -dependent signaling proteins, such as calmodulin and calcineurin. However, it should be noted that cytosolic calcium increase can also activate NMDA receptors via a Ca^{2+} -dependent Src kinase pathway (Nishizuka, 1988; Ben-Ari et al., 1992; Lu et al., 1999). Therefore, one signaling molecule (e.g., Ca^{2+}) can have opposite effects on the same receptors, possibly depending on the intensity and/or timing of the calcium transient. For example, it has been shown that $[\text{Ca}^{2+}]_i > 400$ nM will result in excitotoxicity in neural crest-derived sensory neurons, whereas $[\text{Ca}^{2+}]_i$ between 200 to 400 nM will promote survival in these cells (Johnson et al., 1992). Consistent with

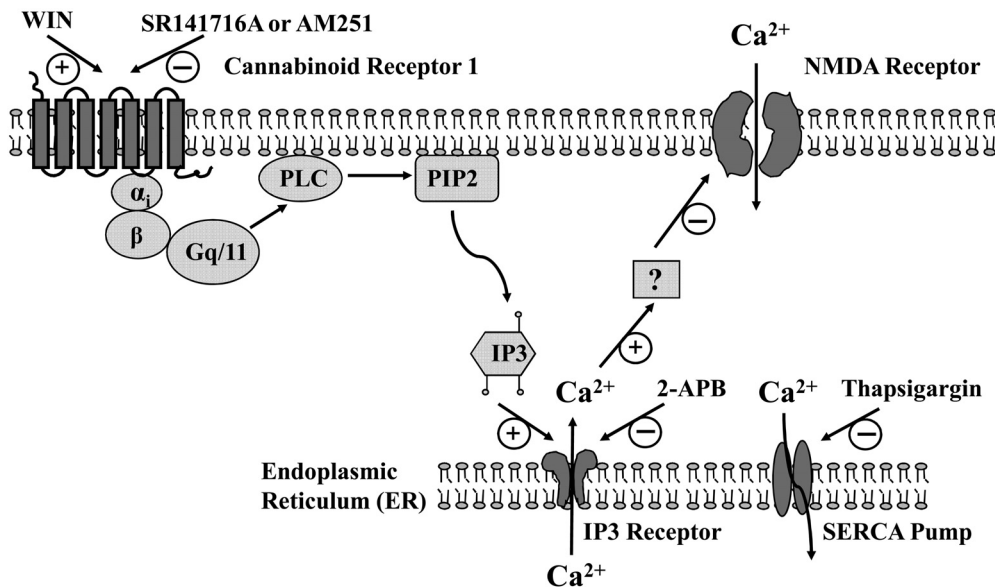


Fig. 9. Schematic illustration of the calcium signaling pathways that are modulated by the cannabinoid system. Activation CB1 receptors mobilizes the IP₃ pathway through a G protein-coupled process. Activation of IP₃ receptors triggers calcium release from intracellular calcium stores, which in turn inhibits calcium influx mediated by activated NMDA receptor channels or by voltage-dependent calcium channels (data not shown). Depletion of intracellular calcium stores by SERCA pump inhibitor or blocking calcium release from intracellular calcium stores by IP₃ receptor inhibitors prevents the cannabinoid from inhibiting the calcium influx related to the excitotoxicity of neurons and development of neuropathic pain. How the calcium release from intracellularly stores leads to the inhibition of NMDA receptors and/or voltage-dependent calcium channels remains to be determined.

the previously published literature, we found that an ~550 nM increase in the [Ca²⁺]_i evoked by NMDA was toxic to both DRG neurons and F-11 cells, but a smaller increase produced by WIN (~350 nM) was not cytotoxic and even protected cells from NMDA-induced cytotoxicity. The temporal pattern of the elevation in the [Ca²⁺]_i can also produce different survival effects. In addition, synaptic transmission in hippocampal neurons could either be enhanced (long-term potentiation) by a brief increase of [Ca²⁺]_i with relatively high magnitude or suppressed (long-term depression) by a prolonged modest rise of [Ca²⁺]_i (Yang et al., 1999). Consistent with this argument is our finding that NMDA-evoked Ca²⁺ influx was inhibited by a short duration (<30 s) and low amplitude increase in [Ca²⁺]_i (<300 nM) induced by WIN but not by a more sustained (>100 s) and higher amplitude (>400 nM) [Ca²⁺]_i rise triggered by thapsigargin. The temporal and spatial characteristics of the Ca²⁺ signals may be related to the differential sensitivities of distinct signaling pathways. For example, short duration and low amplitude Ca²⁺ signals preferably stimulate calcineurin and lead to dephosphorylation of various signaling proteins and subsequent inactivation of NMDA receptors (Tong et al., 1995). In contrast, sustained and spatially diffuse and homogenous Ca²⁺ signals may simultaneously activate both “potentiation” and “depression” pathways that converge upon NMDA receptors, resulting in a cancellation effect (Harvey and Collingridge, 1992; Simpson et al., 1993). The temporal and spatial characteristics of calcium signaling may also be determined by the types of cannabinoid ligands. It has been recently demonstrated that two distinct “endogenous” ligands that differ in their chemical nature (lipid versus peptide) activate the same receptor to initiate distinct signaling pathways (Gomes et al., 2009). It is known that CB1 receptors can couple to different G proteins (Lauckner et al., 2005) and that the same G protein-coupled receptors can activate distinct signaling pathways after activation by different ligands (Drake et al., 2008).

Taken together, the data of this study provided significant insight into the interactions between the cannabinoid system and glutamate receptor activation in DRG neurons through the modulation of cytosolic calcium dynamics and the IP₃

signaling pathway (Fig. 9). Given the fact that the DRG neurons are critical for sensory-motor integration, understanding the mechanisms underlying the cannabinoid protection of these neurons and the mechanisms underlying the cannabinoid-mediated antinociception is necessary for the design of specific and efficacious therapies. Recent studies have demonstrated the neuroprotective potential of cannabinoids in various neurodegenerative diseases, such as multiple sclerosis (Pertwee, 2007) and amyotrophic lateral sclerosis, which are characterized by selective death of spinal neurons (Centonze et al., 2007). Also important is the recent recognition of the role of cannabinoids in antinociception and the cannabinoid system as an emerging target for chronic pain pharmacotherapy (Walker and Hohmann, 2005; Pacher et al., 2006).

Acknowledgments

We thank Dr. Lyle Fox for editorial assistance.

References

- Abood ME, Rizvi G, Sallapudi N, and McAllister SD (2001) Activation of the CB1 cannabinoid receptor protects cultured mouse spinal neurons against excitotoxicity. *Neurosci Lett* **309**:197–201.
- Agarwal N, Pacher P, Tegeder I, Amaya F, Constantin CE, Brenner GJ, Rubino T, Michalski CW, Marsicano G, Monory K, et al. (2007) Cannabinoids mediate analgesia largely via peripheral type 1 cannabinoid receptors in nociceptors. *Nat Neurosci* **10**:870–879.
- Ben-Ari Y, Aniksztejn L, and Bregestovski P (1992) Protein kinase C modulation of NMDA currents: an important link for LTP induction. *Trends Neurosci* **15**:333–339.
- Boyd ST (2006) The endocannabinoid system. *Pharmacotherapy* **26**:218S–221S.
- Centonze D, Rossi S, Finazzi-Agrò A, Bernardi G, and Maccarrone M (2007) The (endo)cannabinoid system in multiple sclerosis and amyotrophic lateral sclerosis. *Int Rev Neurobiol* **82**:171–186.
- Chen J, Lee CT, Errico S, Deng X, Cadet JL, and Freed WJ (2005) Protective effects of Delta(9)-tetrahydrocannabinol against N-methyl-D-aspartate-induced AP5 cell death. *Brain Res Mol Brain Res* **134**:215–225.
- Cruzblanca H, Koh DS, and Hille B (1998) Bradykinin inhibits M current via phospholipase C and Ca²⁺ release from IP₃-sensitive Ca²⁺ stores in rat sympathetic neurons. *Proc Natl Acad Sci U S A* **95**:7151–7156.
- Dedov VN, Mandadi S, Armati PJ, and Verkhratsky A (2001) Capsaicin-induced depolarisation of mitochondria in dorsal root ganglion neurons is enhanced by vanilloid receptors. *Neuroscience* **103**:219–226.
- Di Marzo V and Petrosino S (2007) Endocannabinoids and the regulation of their levels in health and disease. *Curr Opin Lipidol* **18**:129–140.
- Docagne F, Muñetón V, Clemente D, Ali C, Loría F, Correa F, Hernangómez M, Mestre L, Vivien D, and Guea C (2007) Excitotoxicity in a chronic model of multiple sclerosis: neuroprotective effects of cannabinoids through CB1 and CB2 receptor activation. *Mol Cell Neurosci* **34**:551–561.
- Drake MT, Violin JD, Whalen EJ, Wisler JW, Shenoy SK, and Lefkowitz RJ (2008)

- β -Arrestin-biased agonism and β 2-adrenergic receptor. *J Biol Chem* **283**:5669–5676.
- Gomes I, Grushko JS, Golebiewska U, Hoogendoorn S, Gupta A, Heimann AS, Ferro ES, Scarlata S, Fricker LD, and Devi LA (2009) Novel endogenous peptide agonists of cannabinoid receptors. *FASEB J* **23**:3020–3029.
- Hampson AJ, Bornheim LM, Scanziani M, Yost CS, Gray AT, Hansen BM, Leonoudakis DJ, and Bickler PE (1998) Dual effects of anandamide on NMDA receptor-mediated responses and neurotransmission. *J Neurochem* **70**:671–676.
- Harvey J and Collingridge GL (1992) Thapsigargin blocks the induction of long-term potentiation in rat hippocampal slices. *Neurosci Lett* **139**:197–200.
- Howlett AC and Mukhopadhyay S (2000) Cellular signal transduction by anandamide and 2-arachidonoylglycerol. *Chem Phys Lipids* **108**:53–70.
- Iversen L and Chapman V (2002) Cannabinoids: a real prospect for pain relief? *Curr Opin Pharmacol* **2**:50–55.
- Johnson EM Jr, Koike T, and Franklin J (1992) A “calcium set-point hypothesis” of neuronal dependence on neurotrophic factor. *Exp Neurol* **115**:163–166.
- Kim SH, Won SJ, Mao XO, Jin K, and Greenberg DA (2006) Molecular mechanisms of cannabinoid protection from neuronal excitotoxicity. *Mol Pharmacol* **69**:691–696.
- Kotecha SA and MacDonald JF (2003) Signaling molecules and receptor transduction cascades that regulate NMDA receptor-mediated synaptic transmission. *Int Rev Neurobiol* **54**:51–106.
- Kyrozis A, Albuquerque C, Gu J, and MacDermott AB (1996) Ca^{2+} -dependent inactivation of NMDA receptors: fast kinetics and high Ca^{2+} sensitivity in rat dorsal horn neurons. *J Physiol* **495**:449–463.
- Lauckner JE, Hille B, and Mackie K (2005) The cannabinoid agonist WIN55,212-2 increases intracellular calcium via CB1 receptor coupling to Gq/11 G proteins. *Proc Natl Acad Sci U S A* **102**:19144–19149.
- Lauckner JE, Jensen JB, Chen HY, Lu HC, Hille B, and Mackie K (2008) GPR55 is a cannabinoid receptor that increases intracellular calcium and inhibits M current. *Proc Natl Acad Sci U S A* **105**:2699–2704.
- Lu WY, Xiong ZG, Lei S, Orser BA, Dudek E, Browning MD, and MacDonald JF (1999) G-protein-coupled receptors act via protein kinase C and Src to regulate NMDA receptors. *Nat Neurosci* **2**:331–338.
- Marsicano G, Moosmann B, Hermann H, Lutz B, and Behl C (2002) Neuroprotective properties of cannabinoids against oxidative stress: role of the cannabinoid receptor CB1. *J Neurochem* **80**:448–456.
- Matsuda LA, Lolait SJ, Brownstein MJ, Young AC, and Bonner TI (1990) Structure of a cannabinoid receptor and functional expression of the cloned cDNA. *Nature* **346**:561–564.
- Munro S, Thomas KL, and Abu-Shaar M (1993) Molecular characterization of a peripheral receptor for cannabinoids. *Nature* **365**:61–65.
- Netzeband JG, Conroy SM, Parsons KL, and Gruol DL (1999) Cannabinoids enhance NMDA-elicited Ca^{2+} signals in cerebellar granule neurons in culture. *J Neurosci* **19**:8765–8777.
- Nishizuka Y (1988) The molecular heterogeneity of protein kinase C and its implications for cellular regulation. *Nature* **334**:661–665.
- Pacher P, B atkai S, and Kunos G (2006) The endocannabinoid system as an emerging target of pharmacotherapy. *Pharmacol Rev* **58**:389–462.
- Pertwee RG (1997) Pharmacology of cannabinoid CB1 and CB2 receptors. *Pharmacol Ther* **74**:129–180.
- Pertwee RG (2007) Cannabinoids and multiple sclerosis. *Mol Neurobiol* **36**:45–59.
- Pertwee RG and Ross RA (2002) Cannabinoid receptors and their ligands. *Prostaglandins Leukot Essent Fatty Acids* **66**:101–121.
- Qiu Z, Parsons KL, and Gruol DL (1995) Interleukin-6 selectively enhances the intracellular calcium response to NMDA in developing CNS neurons. *J Neurosci* **15**:6688–6699.
- Reichling DB and MacDermott AB (1993) Brief calcium transients evoked by glutamate receptor agonists in rat dorsal horn neurons: fast kinetics and mechanisms. *J Physiol* **469**:67–88.
- Richter F, Meurer BH, Zhu C, Madvedeva VP, and Chesselet MF (2009) Neurons express hemoglobin α and β chains in rat and human brains. *J Comp Neurol* **515**:538–547.
- Shen M and Thayer SA (1998) Cannabinoid receptor agonists protect cultured rat hippocampal neurons from excitotoxicity. *Mol Pharmacol* **54**:459–462.
- Simpson PB, Challiss RA, and Nahorski SR (1993) Involvement of intracellular stores in the Ca^{2+} responses to N-methyl-D-aspartate and depolarization in cerebellar granule cells. *J Neurochem* **61**:760–763.
- Tong G, Shepherd D, and Jahr CE (1995) Synaptic desensitization of NMDA receptors by calcineurin. *Science* **267**:1510–1512.
- van der Stelt M and Di Marzo V (2005) Cannabinoid receptors and their role in neuroprotection. *Neuromolecular Med* **7**:37–50.
- Van Sickle MD, Duncan M, Kingsley PJ, Mouihate A, Urbani P, Mackie K, Stella N, Makriyannis A, Piomelli D, Davison JS, et al. (2005) Identification and functional characterization of brainstem cannabinoid CB2 receptors. *Science* **310**:329–332.
- Walker JM and Hohmann AG (2005) Cannabinoid mechanisms of pain suppression. *Handb Exp Pharmacol*. **168**:509–554.
- Woolf CJ (1983) Evidence for a central component of post-injury pain hypersensitivity. *Nature* **306**:686–688.
- Woolf CJ and Salter MW (2000) Neuronal plasticity: increasing the gain in pain. *Science* **288**:1765–1769.
- Yang SN, Tang YG, and Zucker RS (1999) Selective induction of LTP and LTD by postsynaptic $[Ca^{2+}]_i$ elevation. *J Neurophysiol* **81**:781–787.
- Yankura K, Zhang HY, and Bhat MB (2003) Role of vanilloid receptor in the capacitative calcium entry in sensory neurons. *Anesthesiology* **99**:A764.
- Zhang J, Hoffert C, Vu HK, Groblewski T, Ahmad S, and O’Donnell D (2003) Induction of CB2 receptor expression in the rat spinal cord of neuropathic but not inflammatory chronic pain models. *Eur J Neurosci* **17**:2750–2754.
- Zhuang SY, Bridges D, Grigorenko E, McCloud S, Boon A, Hampson RE, and Deadwyler SA (2005) Cannabinoids produce neuroprotection by reducing intracellular calcium release from ryanodine-sensitive stores. *Neuropharmacology* **48**:1086–1096.

Address correspondence to: Dr. Jianguo Cheng, Department of Pain Management/C25, Cleveland Clinic, 9500 Euclid Avenue, Cleveland, OH 44195. E-mail: chengj@ccf.org
